

Biobased Composite Resins Design for Electronic Materials

Mingjiang Zhan, Richard P. Wool

Department of Chemical Engineering and Center for Composite Materials, University of Delaware, Newark, Delaware 19716

Received 24 November 2009; accepted 13 April 2010

DOI 10.1002/app.32633

Published online 13 July 2010 in Wiley InterScience (www.interscience.wiley.com).

ABSTRACT: Biobased materials developed from triglycerides contain a large variety of structures, which makes it difficult to predict their properties. In this study, we used a structure–property relation to design biobased materials, both theoretically and experimentally. A general equation to predict the crosslink density in terms of the level of chemical functionalities of the triglycerides was derived and used as a design rule for high-crosslinked polymer materials. The twinkling fractal theory and the Clausius–Mossotti equation were used to guide two approaches of synthesis to improve the properties of the biobased thermosets: the biobased resin acrylated epoxidized soybean oil (AESO) was either crosslinked with divinylbenzene (DVB) or chemically modified by phthalic anhydride. The DVB-crosslinked resins had a 14–24°C increase in their

glass-transition temperatures (T_g 's), which was dependent on the crosslink densities. T_g increased linearly as the crosslink density increased. Phthalated acrylated epoxidized soybean oil (PAESO) had an 18–30% improvement in the modulus. The dielectric constants and loss tangents of both DVB-crosslinked AESO and PAESO were lower than conventional dielectrics used for printed circuit boards (PCBs). These results suggest that the new biobased resins with lower carbon dioxide footprint are potential replacements for commercial petroleum-based dielectric materials for PCBs. © 2010 Wiley Periodicals, Inc. *J Appl Polym Sci* 118: 3274–3283, 2010

Key words: crosslinking; dielectric properties; glass transition; renewable resources

INTRODUCTION

With the price of petroleum-based materials generally increasing, biobased materials have drawn significant attention from researchers. Unlike petroleum-based materials, which have created many environmental concerns,¹ polymeric materials developed from renewable resources, such as plant oils, proteins, and starch, have both economic and environmental advantages. Soybean oil, mainly composed of triglyceride molecules, is among those inexpensive natural resources that can be a replacement for petroleum-based polymeric materials after polymerization. Although pure unsaturated triglycerides can undergo cationic polymerization, the rate of polymerization is relatively slow.² Therefore, the chemical functionality necessary for fast free-radical polymerization is added to the triglyceride molecules. The Affordable Composites from Renewable Resources (ACRES) group at the University of Delaware has done extensive research on the incorporation of

polymerizable groups into the active sites of triglycerides.^{3–7} Among those modified triglycerides, acrylated epoxidized soybean oil (AESO) was proposed as a replacement for epoxy resins for printed circuit board (PCB) applications.⁸ Although AESO has some promising properties, its glass-transition temperature (T_g) is relatively low, and its mechanical properties have to be improved for PCB applications. There have been several studies in recent years on the improvement of the properties of AESOs in which (1) AESO was mixed with styrene to improve the processability, and the T_g of the resins copolymerized with styrene was significantly higher because the aromatic nature of styrene imparted rigidity to the network and (2) maleic anhydride and bisphenol A were also reacted with triglyceride to increase the rigidity of the resin system.⁵

The reaction products of triglyceride molecules are complicated and involve a mixture of different fatty acids with a large variety of structures; this makes it difficult to predict their properties. The lack of theoretical guidelines for the triglyceride molecule design requires significant work on product development. Thus, a good understanding of the structure–property relation is necessary, both theoretically and experimentally. Wool and Sun⁹ adopted percolation theory to predict T_g in polymer thin films and bulk, which could be used to guide the design of the triglyceride resins for different

Correspondence to: R. P. Wool (wool@udel.edu).

Contract grant sponsor: United States Department of Agriculture-Cooperative State Research, Education, and Extension Service-National Research Initiative (USDA-CSREES-NRI); contract grant number: 2005-35504-16137.

applications. The linear relation between the crosslink density and T_g was derived to predict T_g . On the basis of these, the twinkling fractal theory (TFT)^{10,11} was developed to predict different properties, such as T_g and yield stress, of polymers. For other important properties for an electronic material, such as the dielectric properties, Debye¹² derived the Clausius–Mossotti equation and related the dielectric constant (ϵ) to the microscopic quantity of the molecules; the resulting equation could be used to design a molecule with a desired ϵ .

In this study, a general equation to predict the crosslink density in terms of the level of chemical functionalities of the triglycerides was derived and used as a design rule for high-crosslinked polymer materials. TFT and Debye's equation were used to guide the approaches of synthesis to improve the properties of the biobased thermosets: the biobased resin AESO was either crosslinked with divinylbenzene (DVB) or chemically modified by phthalic anhydride (PA). The approaches were adopted to demonstrate that a well-understood structure–property relation can help to design a greener biobased material for certain applications. For example, in this study, the material developed was intended to be used in the PCB industry. The thermomechanical and dielectric properties were also thoroughly studied for the new resins developed in this study.

EXPERIMENTAL

Materials

AESO (trade name Ebecryl 860) was purchased from Cytec Industries (Smyrna, GA). DVB and the thermal initiator *n-tert*-butyl peroxybenzoate were obtained from Aldrich (Milwaukee, WI). PA, styrene, hydroquinone, *N,N*-dimethylbenzylamine, and chloroform-*d* (CDCl_3) were purchased from Sigma (St. Louis, MO). All materials were used as received.

Preparation of DVB-crosslinked AESO

The AESO resin was mixed with styrene and DVB. The weight ratio of AESO to styrene was 70 : 30. The amounts of DVB were varied. The nomenclature adopted in this study for the DVB-crosslinked AESO was based on the composition of the monomers. For example, AESO70–STY30–DVB5 represents a thermoset prepared from AESO, styrene, and DVB with weight ratio of 70 : 30 : 5.

Phthalation of AESO

Certain amounts of AESO and 0.1 wt % hydroquinone were first added to the reaction vessel and heated to 100°C at a heating rate of 2–3°C/min with

stirring. The necessary amount of PA was ground to a fine powder and then added to the AESO mixture at 100°C. The mixture was then heated to 135–140°C, at which the PA was dissolved to form a homogeneous solution. The *N,N*-dimethylbenzylamine catalyst was then added to the vessel in the amount of 2 wt % of AESO. The reaction was stopped after 6 h. During the procedure, nitrogen gas was used for purging and the removal of water out of the reaction products, if water existed.

Throughout the procedure, samples of the reaction mixture were taken at 1-h intervals. These samples were taken from the reaction vessel with Pasteur pipettes for ¹H-NMR analysis. The analysis was done to examine the reaction progress as a function of time.

The resulting phthalated acrylated epoxidized soybean oil was named PAESO; for the different amounts of PA added to the reaction, a numerical number was added after PAESO. For example, PAESO2 represents PAESO with a molar ratio of PA to AESO in the reactant mixture of 2 : 1.

Free-radical polymerization

The free-radical polymerization of soy-oil-derived resins was carried out at elevated temperatures from 90 to 120°C. *N-tert*-Butyl peroxybenzoate was added as an initiator in the amount of 1.5 wt %. To prevent oxygen inhibition, the resin was degassed in a vacuum oven before curing. The resin was cured at 90°C for 2 h, followed postcuring at 120°C for 2 h. After the cure cycle was completed, the samples were cut and polished for various tests.

Characterization

¹H-NMR was used to monitor the phthalation reaction. The samples were prepared by the dissolution of 60 mg of the sample in 0.6 mL of chloroform-*d*. A Bruker AV400 spectrometer (Bruker, Germany) was used to analyze the samples. A pulse width of 90° was used for all of the samples. The samples were analyzed at 20°C, and 16 scans of each sample were taken.

The storage modulus and T_g of the polymer were measured with a dynamic mechanical analyzer (DMA 2980, TA Instruments, New Castle, DE) at a heating rate of 2°C/min according to ASTM D 5023. T_g was obtained from the temperature at which the maximum value of the loss factor ($\tan \delta$) occurred.

The dielectric properties of the materials were measured on an impedance analyzer (HP 4294A, Agilent Technologies, Santa Clara, CA) at frequencies from 10 kHz to 5 MHz. The diameter of a sample was 10 mm, and the thickness was 5 mm.

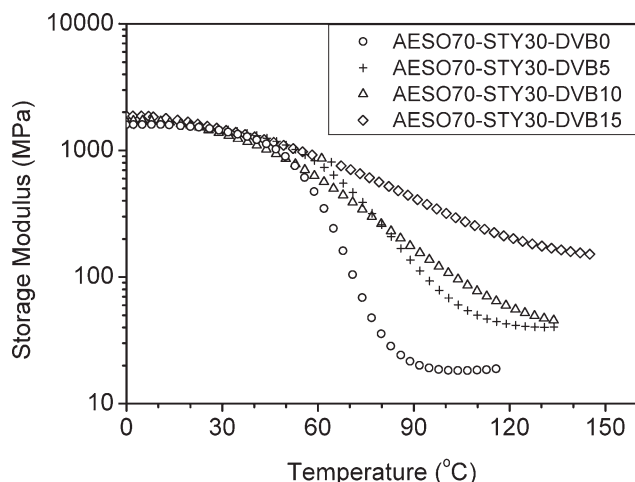


Figure 1 Temperature dependence of the storage moduli of DVB-crosslinked AESO. The addition of DVB increased the storage modulus of the DVB-crosslinked AESO and broadened the glass-transition region.

The viscosity of the biobased resin was measured with a TA Instruments (New Castle, DE) AR-G2 rheometer. A cone plate 40 mm in diameter and with a cone angle of 4° was used for all of the samples. The samples were first equilibrated at 20°C , and then, the temperature was increased to 70°C at a heating rate of $1^\circ\text{C}/\text{min}$, with a shear rate of 1 s^{-1} . A repeat run was performed for all samples.

The molecular weight distribution of the resin was measured by gel permeation chromatography (GPC; Waters 2695, Milford, MA). A Waters 2414 refractive-index detector and a $7.8 \times 300\text{ mm}^2$ Styragel column (Waters) were used.

Soxhlet extraction by methylene chloride was done to determine the gel fractions of the thermosets. A 2-g sample of the cured polymer was extracted for 24 h with 100 mL of refluxing methylene chloride with a Soxhlet extractor. (Soxhlet extractor was named after Franz von Soxhlet. The extractor was purchase from ACEGLASS, Vineland, NJ). After extraction, the insoluble solid was dried at 50°C *in vacuo* for 4 h before it was weighed. The gel fraction was determined from the weight ratio of the extracted sample to its weight before extraction.

RESULTS AND DISCUSSION

The two different chemical modification approaches are analyzed and discussed in the following two separate subsections.

DVB-crosslinked AESO

Dynamic mechanical analysis (DMA)

Li et al.¹³ obtained hard plastics from the copolymerization of soybean oils and DVB. However, the plas-

tics were very brittle because of their high crosslink density and nonuniform crosslink structure. After other comonomers, such as styrene, were added, the mechanical properties of the resulting plastics were significantly improved.² In the same manner, styrene was used as a comonomer in this study to improve the mechanical properties.

The storage moduli of the crosslinked AESOs are shown in Figure 1. The storage modulus initially remained almost constant at low temperatures. As the temperature increased, there was a sharp drop in the temperature region between 50 and 100°C , which indicated that a glass transition occurred at this temperature range. The drop in the modulus corresponded to the onset of segmental mobility of the polymer network, where the chains of the amorphous polymer began to coordinate large-scale motions, in other words, the amorphous regions began to melt. After the glass transition, the rubbery modulus plateau was reached, where the polymer behaved like a rubber. For a thermosetting polymer, the plateau region continues until the sample begins to degrade because the crosslinks prevent the chains from slipping past one another.¹⁴ Clearly, with increasing DVB, the storage modulus at the plateau region increased; thus, the crosslinking density increased. Figure 1 also shows that the glass-transition range broadened when the amount of DVB increased in the polymer, as the curves started to overlap. This was because the additional crosslinks increased segmental heterogeneities and, thus, broadened the glass-transition region.¹⁵

Figure 2 shows $\tan \delta$ of the DVB-crosslinked AESO by DMA. The peaks of the $\tan \delta$ corresponded to the α relaxation, that is, T_g of the crosslinked polymers and were, thus, used to determine the T_g values of the polymers. With increasing amount of

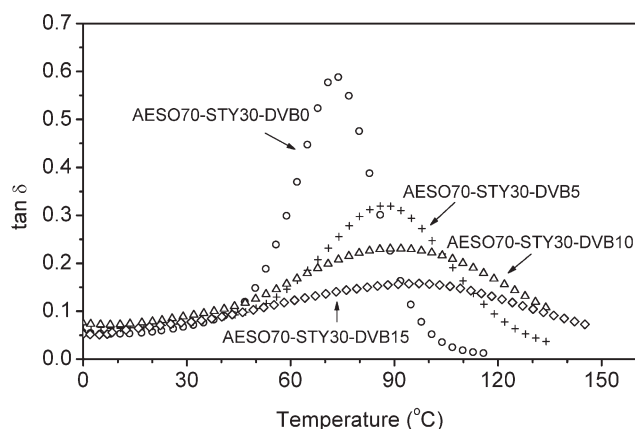


Figure 2 Temperature dependence of $\tan \delta$ of DVB-crosslinked AESO. The shift of the peak to the high-temperature side indicates the increasing T_g with the addition of DVB in the resin. The span of the glass-transition region also increased with increasing DVB content.

DVB in the resin, the peak of $\tan \delta$ shifted to a higher temperature; this indicated a higher T_g . This was because crosslinking hindered the motion of the polymer segments; thus, a higher temperature was required for the onset of the motion. The DVB-crosslinked AESO resins had a 14–24°C increase in their T_g values, which was dependent on the DVB content. As the DVB content increased, the $\tan \delta$ peak value decreased because of the higher crosslinking density and lower intersegmental and intrasegmental friction coefficients. In addition to reducing the peak values, the higher crosslinking density also increased segmental heterogeneities and, thus, broadened the $\tan \delta$ region, which was consistent with the storage modulus analysis. Thus, the DVB content between AESO70–STY30–DVB10 and AESO70–STY30–DVB15 was recommended to obtain a high T_g but maintain a relatively narrow glass transition. An increase in T_g has also been reported for other AESO polymers as the level of acrylation increased for triglyceride-based polymers, both with and without comonomers.^{16,17}

Crosslink density

The plateau modulus determined from DMA above T_g is a measure of the effective crosslink density of polymers. The crosslink density of a polymer can be determined from the theory of rubber elasticity by the following equation:¹⁸

$$E = 3\nu RT \quad (1)$$

where ν is the crosslink density and E is the elastic modulus of the polymer in the plateau region above T_g . T is the temperature where the plateau region is reached; in this study, $T_g + 40$ (K) was used in the calculations. R is the ideal gas constant (8.314 J K⁻¹ mol⁻¹), and T is the absolute temperature (K).

In theory, we define *crosslinks* as the chains that connect two infinite polymer chains. The number of crosslinks in the network composed of n crosslink agents can be expressed as a function of the composition and the functionality of each component in the resin, such as the triglycerides, by eq. (2):

$$\nu = \sum_{i=1}^n \frac{3\rho w_i (f_i X_i - 1)}{MW_i} \quad (2)$$

where ρ is the density of the polymer, w is the weight fraction of the multifunctional components in the resins, f is the number of polymerizable groups (e.g., C=C double bonds in this study) in the monomer molecule, X is the extent of polymerization, MW is the molecular weight of each monomer, and the subscript i denotes i th component in the resin.

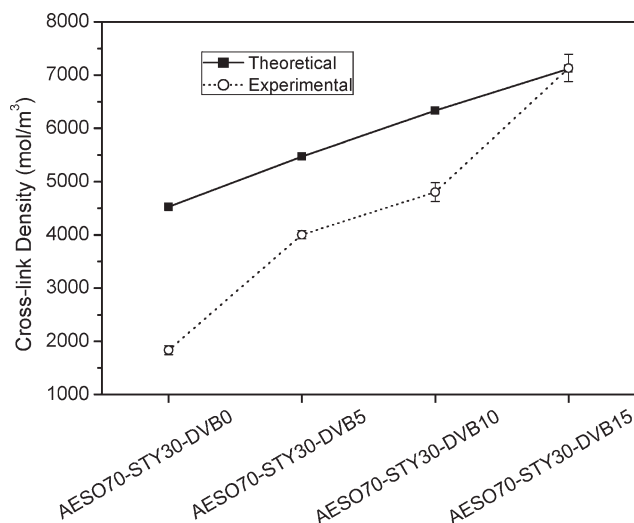


Figure 3 Theoretical and experimental crosslink density of DVB-crosslinked AESO with different amounts of DVB. The experimental values were lower than the theoretical values because of the internal cyclization and plasticization effect.

The AESO resin contained 3.4 acrylates per triglyceride,¹⁹ that is, 3.4 double bonds. The number of double bonds in DVB was 2. These numbers were used as f in eq. (2) to calculate the crosslink density of the polymer. According to La Scala,¹⁶ the extent of the reaction was 0.99 for acrylate groups. The molecular weight of AESO was 1186 g/mol, and the density of the cured polymers was 1080 kg/m³.

According to eq. (2), we could define the effective functionality that contributed to the polymer network as $(f_i X_i - 1)/MW_i$. AESO had 3.4 double bonds, so it also served as a crosslink agent. However, because of its high molecular weight, it had a much lower effective functionality than DVB (1 : 3.78, with X assumed to be 100%). Thus, the addition of DVB increased the crosslink density of the polymer network.

Figure 3 shows the crosslink densities of the DVB-crosslinked AESO calculated by eq. (2) and the values determined experimentally. The crosslink density of the thermosets increased as the amount of DVB in the resin increased because of the higher effective functionality of DVB. The results show that the theoretical crosslink densities were higher than the experimental values because of two reasons: (1) the internal cyclization reaction (monomer units incorporated into the polymer losing their pendent vinyls by cyclization within their own primary polymerization chain²⁰) of triglycerides and DVB^{16,17} and (2) the plasticization effect by saturated fatty acids, which underestimated the crosslink densities experimentally during DMA.^{13,19}

The internal cyclization resulted in small molecules that were not connected to the thermoset network. The fraction of network could be determined by Soxhlet extraction (see Table I). After Soxhlet

TABLE I
Contents of the Crosslinked Fractions, Crosslink Densities, and T_g Values of the DVB-Crosslinked Polymers

Polymer	Contents of the crosslinked polymer (wt %)	Crosslink density (mol/m ³)	T_g (K)
AESO70-STY30-DVB0	94.09	1833 ± 85	346.0 ± 0.7
AESO70-STY30-DVB5	97.04	4003 ± 77	359.8 ± 0.6
AESO70-STY30-DVB10	94.50	4802 ± 176	363.2 ± 0.7
AESO70-STY30-DVB15	97.68	7133 ± 256	369.0 ± 2.3

extraction, the soluble part of the polymer was the relatively small molecules created by internal cyclization, and the insoluble part was the polymer network. The crosslinked fraction of the polymer varied from 94.1 to 97.7 wt % and was much higher than the values reported by Li et al.¹³

Given the adjusted factor to account for the cyclization reactions, the total crosslink density for a polymer network is given by

$$v = \sum_{i=1}^n \frac{3\rho w_i [(f_i - f_c)X_i - 1]}{MW_i} \quad (3)$$

where f_c is the number of functional groups lost toward intramolecular cyclization.

According to eq. (3), during the polymerization the numbers of acrylate groups lost per triglyceride toward intramolecular cyclization for the four polymers were 1.3, 0.8, 0.8, and 0, respectively.

Effect of the crosslink density on T_g

Several different models have been developed to predict the effect of the degree of crosslinking on T_g .^{21–24} These models predict T_g as a function of crosslink density quite well for homopolymerized triglycerides.¹⁶ For example, the prediction for the dependence of T_g on crosslink density (v) is given by the TFT of T_g .^{10,11}

$$T_g(v) = T_g^0 + \frac{T_g^0 M_{ox}}{\rho(1 - p_c)} v \quad (4a)$$

where T_g^0 is the glass-transition temperature of the linear polymer extrapolated to $v = 0$, M_{ox} is the molecular weight per backbone atom of the crosslink chain structure, and $p_c \approx 0.5$ is the vector percolation threshold when the glassy modulus approaches zero.

According to TFT, the T_g is linearly dependent on the crosslink density. Figure 4 shows the T_g of the crosslinked polymer as a function of the crosslink density. As the crosslink density increased, T_g of the polymer increased linearly. Because of the higher segmental heterogeneity at higher crosslink densities, AESO70-STY30-DVB15 had a higher variance. The fitted equation is given by

$$T_g(\text{K}) = 340 + 0.00406v \quad (4b)$$

ε values and molecular structure

Dielectrics are the major material for electronic packaging. The performance of the electric signal in a PCB is mostly limited by the interlayer capacitance, which is dictated primarily by ε of the packaging materials. It is well known that the signal delay time (t_d) behaves as $t_d \propto \sqrt{\varepsilon}$, such that a low ε promotes a high signal speed. A decrease in the ε values also minimizes the crosstalk effects between signal lines.²⁵ The ratio of the imaginary part to real part of the ε values, known as the *dissipation factor* or *loss tangent*, is also a critical value for PCB. A low value of the loss tangent will reduce the power consumption, which is favorable for high-speed applications.^{25,26} Thus, a lower ε material is most desirable for PCB applications.

Figure 5 shows the ε values and loss tangents of the DVB-crosslinked polymers measured at room temperature at 1 MHz. The ε values decreased from 3.77 to 3.62 with the addition of DVB in the resin. The loss tangent of the polymers was about 0.02 for all of the samples, indicating very low energy (signal) loss.

The ε values of the biobased materials were lower than the values of the most widely used epoxy resins, which had ε values of 4.2–4.7. It was also similar to other resins used in dielectric applications, such

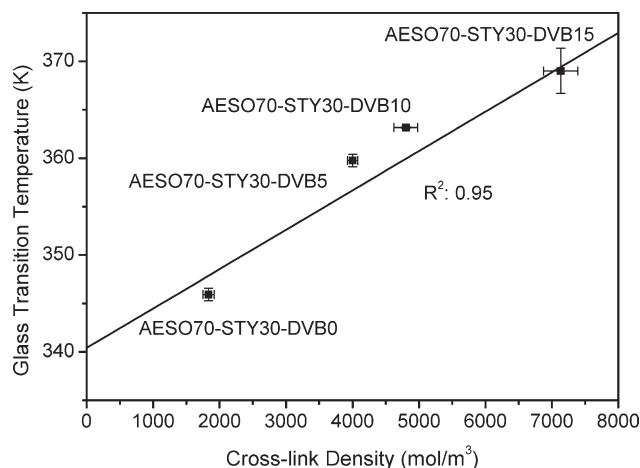


Figure 4 Relation of T_g and the crosslink density. T_g increased linearly as the crosslink density of the polymer increased. The measurement errors were used for direct weighing for the linear fit.

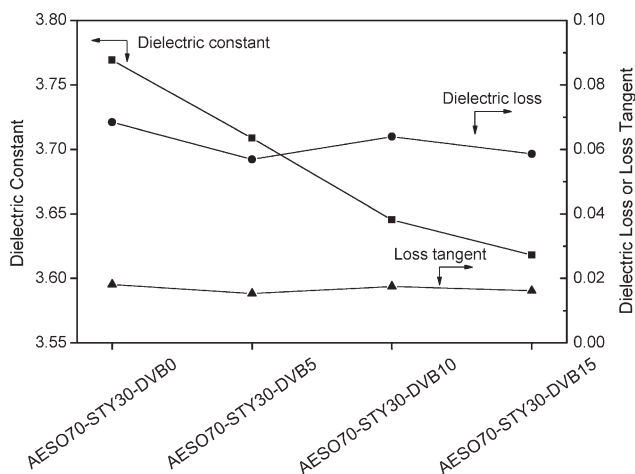
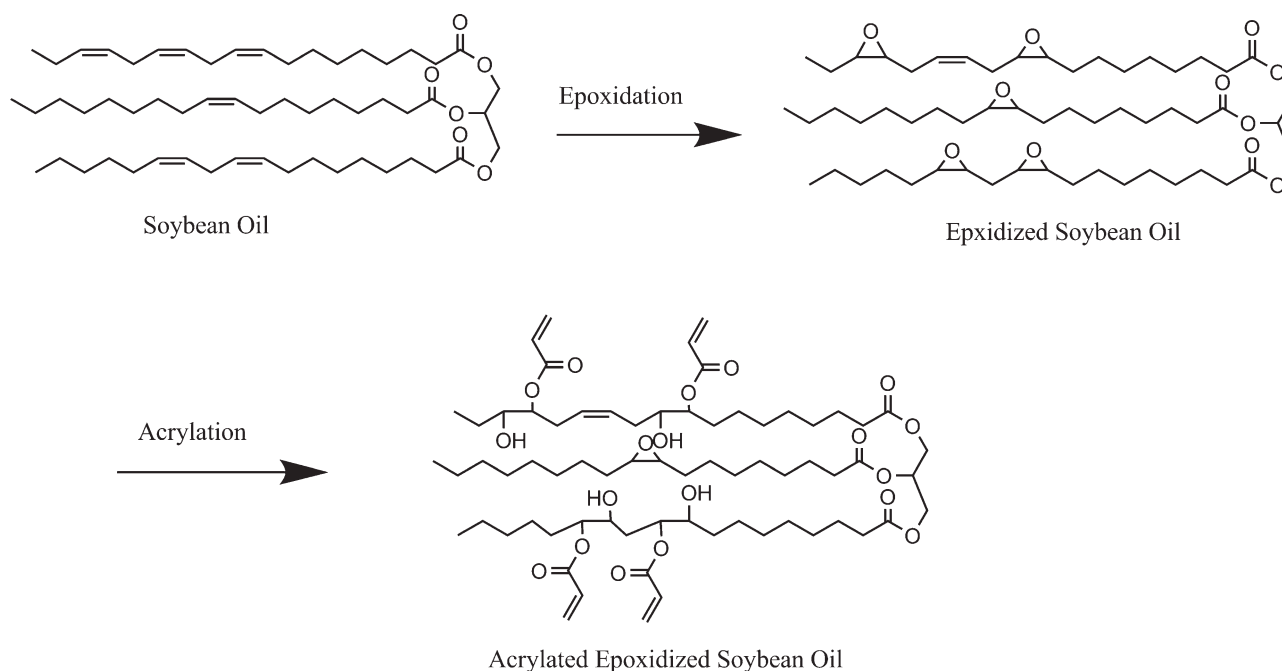


Figure 5 ϵ and loss tangent of the DVB-crosslinked AESO measured at 1 MHz and room temperature. The addition of DVB decreased ϵ of the DVB-crosslinked AESO because of its lower polarity.

as polyimides and polyesters. The lowest ϵ was 1, which was *in vacuo* or closely in air. Combined with chicken feather fibers, which have air in their hollow structure, the resulting composites had lower ϵ values and could be a substitute for petroleum-based resins in many electronic material applications.^{8,27}

ϵ , which is a macroscopic quantity, can be related to the microscopic quantity of the molecules by the Clausius–Mosotti's equation, derived by Debye:¹²

$$\frac{\epsilon - 1}{\epsilon + 2} = \frac{4\pi \rho}{3M} N_A \left(\alpha + \frac{\mu^2}{kT} \right) \quad (5)$$



Scheme 1 Modification of soybean oil (triglyceride) by epoxidation and acrylation reactions. The double bonds in the acrylate groups of acrylated epoxidized soybean oil were ready for free-radical polymerization.

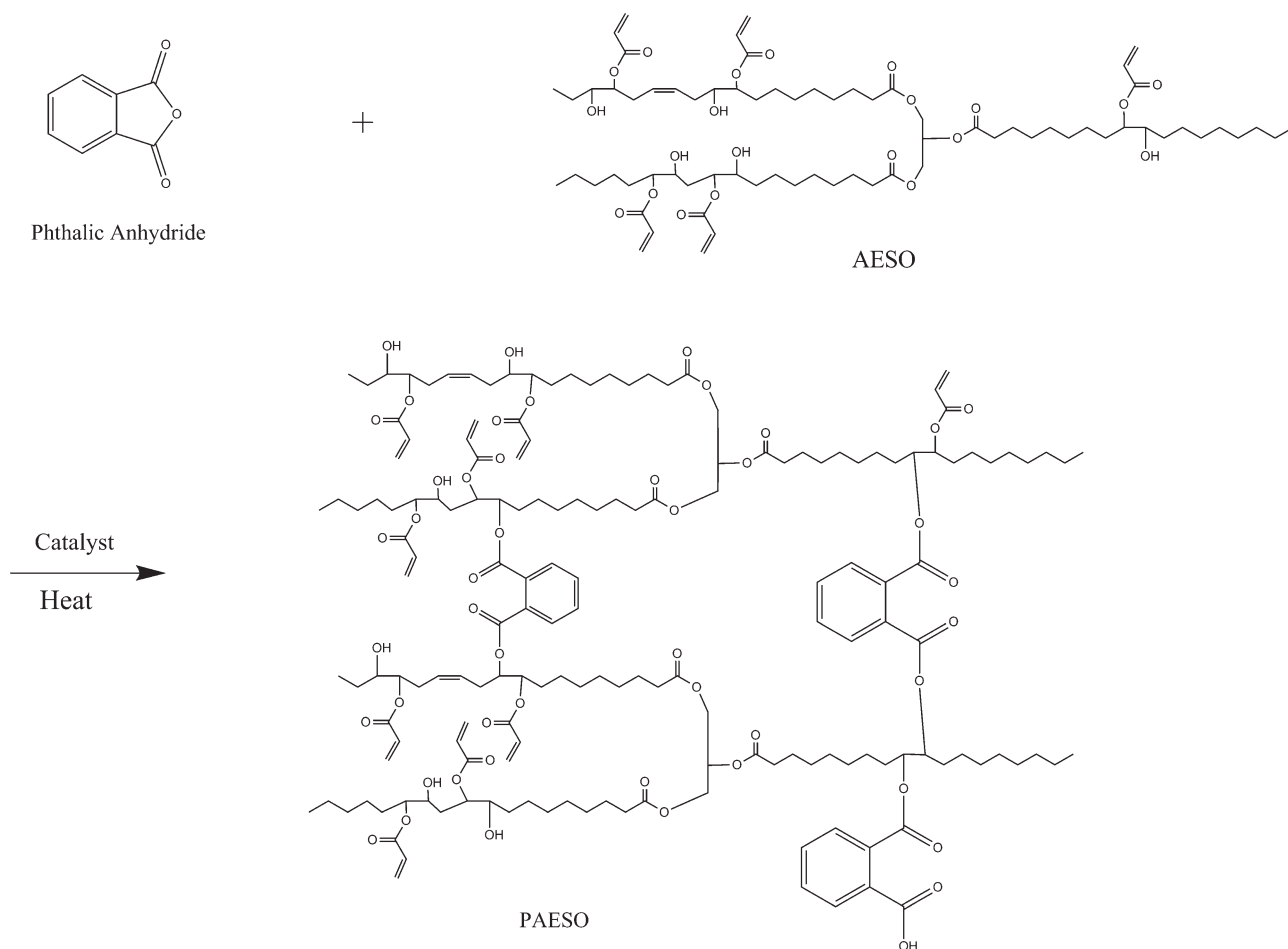
where α is the polarizability of chemical bonds; μ is the dipole moment of the molecule, which depends on the frequencies; M is the molecular weight of the material; N_A is Avogadro's number; and k is Boltzmann's constant.

Although this equation was designed for predicting the ϵ values of liquids and gases, it is also useful for qualitatively analyzing the ϵ values of the polymer.²⁸ This can be used to guide the selection of monomers for electronic applications. With the addition of more groups with low polarity in a system, ϵ of the resin decreases. Thus, nonpolar groups, such as C–C bonds and C–H are desirable. For example, ϵ of polyethylene is about 2.3.²⁹ Also, the aromatic ring is nonpolar and will reduce ϵ and impart rigidity to a polymer. With more DVB in our system, ϵ of the resin decreased because of the reduced molecular mobility. The polarity of the C–C bonds and C–H was low, and the benzene ring was nonpolar; this made α smaller and, hence, ϵ smaller. The low polarity of the resin also controlled the loss tangent in the low-value range.

PAESO and its polymer

Phthalation reaction

AESO had 3.4 acrylate groups that could be used for free-radical polymerization. When epoxidized soybean oil was converted to AESO (see Scheme 1), every single acrylate group obtained gave a hydroxyl group on the AESO molecule. These hydroxyl groups remained unreacted after the thermoset was



Scheme 2 Phthalation of AESO with PA. PA reacted with OH groups on the AESO molecules and formed intermolecular chemical bonds.

cured. Different approaches have been used to use this functional group to improve the properties of triglyceride resins. Can et al.⁵ used maleic anhydride to react with the alcoholysis (glycerolysis or pentaerythritolysis) products of soybean oil. However, Lu et al.³⁰ used maleic anhydride to react with AESO directly. The resulting maleated soy resins had higher T_g values (up to 165°C) and storage moduli (up to 3 GPa) than AESO.

In this study, PA was used to phthalate AESO by addition to the OH group, where new crosslink sites formed accordingly, as shown in Scheme 2. The incorporation of PA into the resin should have also increased the rigidity of the polymer network because of its aromatic nature.

La Scala¹⁶ systematically studied the NMR analysis of triglycerides and chemically modified triglycerides, and the corresponding peak assignment was used in this study. Figure 6 shows the NMR spectra of the products of the phthalation reaction. PA attached to an AESO molecule (7.25 ppm) was assigned as peak 1, and free PA (double peaks around 8 ppm) was assigned as peak 2. As the reaction time increased, the ratio of reacted PA to free

PA increased. On the basis of NMR, the conversion of AESO to PAESO was calculated. The methyl protons at the end of fatty acids (0.9 ppm) were used as internal standards to determine the extents of the reaction. The calculated numbers of PA added to AESO are shown in Table II. The conversion of PA decreased as the amount of PA increased, and it did not reach 100%, even when we extended the reaction

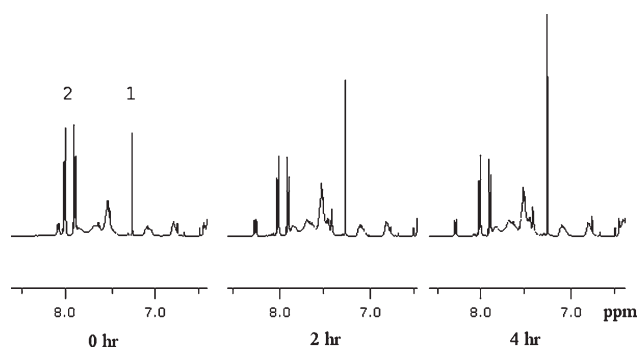


Figure 6 $^1\text{H-NMR}$ spectra of the phthalation reaction of AESO and PA. As the reaction time increased, the ratio of reacted PA (peak 1) to free PA (peak 2, double peaks) increased.

TABLE II
Molecular Weights, Conversions, and Amount of Phthalates Formed in the Phthalation Reaction of AESO

Molar ratio (AESO : PA)	Weight ratio (AESO : PA)	Phthalates added per AESO	Conversion of PA (%)	M_n	Weight-average molecular weight	PDI	Oligomer units
1 : 1	100 : 12.34	0.9	90	6385	12,321	1.93	5.3
1 : 2	100 : 24.68	1.6	80	7344	18,115	2.47	6.1
1 : 3	100 : 37.02	1.7	57	7393	18,465	2.50	6.2

time. An equilibrium was reached for this reaction, which was similar to the reaction of maleic anhydride with AESO.¹⁶ As the ratio of PA to AESO increased, the number of PA added to AESO did not increase proportionally. Only 1.7 PA molecules were reacted with AESO when the ratio of PA to AESO was 3.

Molecular weight distribution of PAESO

Figure 7 shows the molecular weight distribution of the different PAESOs synthesized from the phthalation reaction. The large peaks at 17.5 min indicated that some AESO remained unreacted for all of the phthalation reactions. The average molecular weight of AESO was 1186 g/mol, and that of PA was 148 g/mol. As each PA only reacted with one AESO molecule, the resulting molecular weight of PAESO was about 1690 g/mol if all of the hydroxyl groups reacted with PA. However, the GPC results showed a considerable amount of molecules with large molecular weight (2500–31,000 g/mol) in the products; this indicated that intermolecular bonds between AESO molecules formed. The average molecular weights are shown in Table II. The PAESOs had high polydispersity index (PDI) values, that is, wide molecular weight distributions. The number-average molecular weights (M_n 's) were 6385, 7344, and 7393, respectively; this meant that oligomerization occurred during the reac-

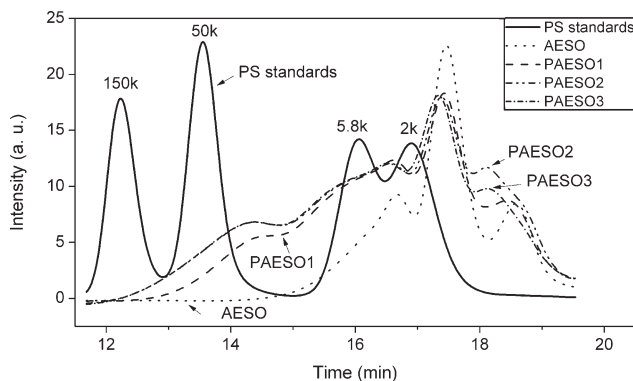


Figure 7 GPC of AESO and PAESO. Different sizes of polystyrene (PS; molecular weights = 2, 5.8, 50, and 150, PDI < 1.03) were used as standards, and AESO was used as a control. PAESO2 and PAESO3 had similar molecular weight distributions, and their molecular weights were larger than those of PAESO1 and AESO.

tion, as we expected (see Scheme 2). On the basis of M_n , the average AESO units of each oligomer for PAESO1, PAESO2, and PAESO3 were 5.1, 6.1, and 6.2, respectively. Interestingly, PAESO2 and PAESO3 had very similar molecular weight distributions, which indicated that, in this reaction, the additional PA as a reactant did not react with AESO when the molar ratio of PA to AESO was greater than 2 : 1.

Rheology of PAESO

The effect of the temperature on the viscosity of the triglyceride-based crosslinkers is shown in Figure 8. With the formation of oligomers in the final product (Table II), the high molecular weight of PAESO resulted in a high viscosity. The initial viscosity of PAESO was so high that it had to be mixed with 30 wt % styrene before it was measured.

The Arrhenius model could be used to fit the viscosity (η) as a function of temperature:

$$\eta = \eta_0 \exp\left(-\frac{E_\eta}{RT}\right) \quad (6a)$$

where η_0 is the prefactor and E_η is the activation energy for the viscous liquid (J/mol).

The calculated activation energy was 41.1 kJ/mol. Thus, the data in Figure 8 could be calculated by

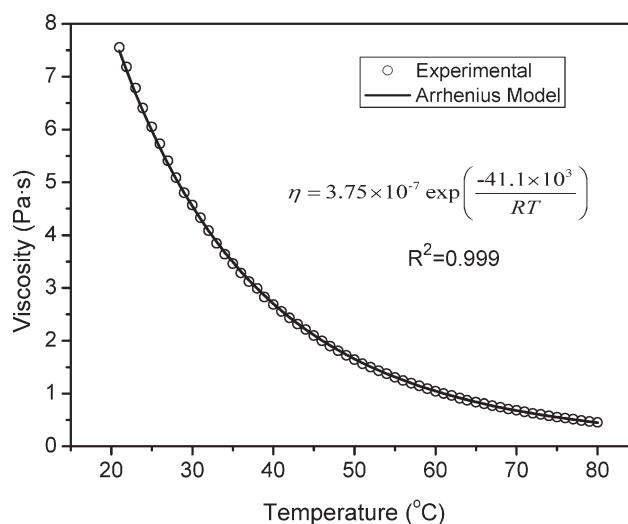


Figure 8 Viscosity of PAESO2 (with 30 wt % styrene) as a function of the temperature. The Arrhenius model could be used to predict the experimental data.

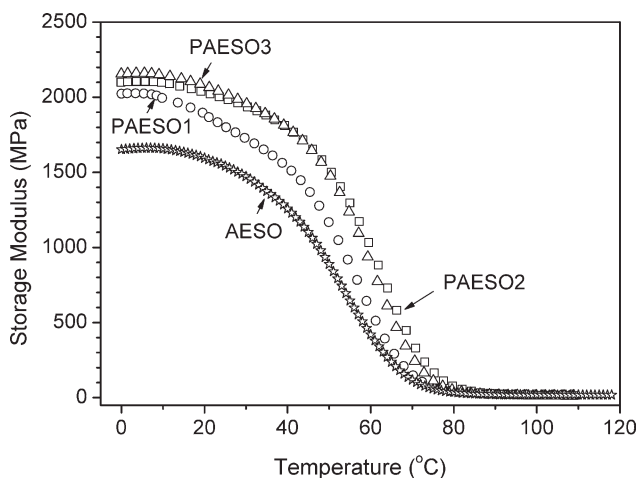


Figure 9 Temperature dependence of the storage moduli of AESO and PAESO. The incorporation of PA increased the modulus. The moduli of (\square) PAESO2 and (\triangle) PAESO3 were very close but higher than that of (\circ) PAESO1.

$$\eta = 3.75 \times 10^{-7} \exp\left(\frac{-41.1 \times 10^3}{RT}\right) \quad (6b)$$

DMA of PAESO

Figure 9 illustrates the temperature dependence of the storage moduli of different PASEOs obtained from the phthalation reactions. The storage moduli of the AESO and PAESOs were similar in nature. The modulus remained high at room temperature, then dropped sharply from 30 to 70°C, and finally reached the rubbery plateau region. The moduli of the PAESOs were higher than that of AESO in the whole glassy state, which proved that incorporation of PA to AESO increased the rigidity of the resin and thus increased the modulus. The storage moduli of PAESO2 and PAESO3 were very close but higher than PAESO1

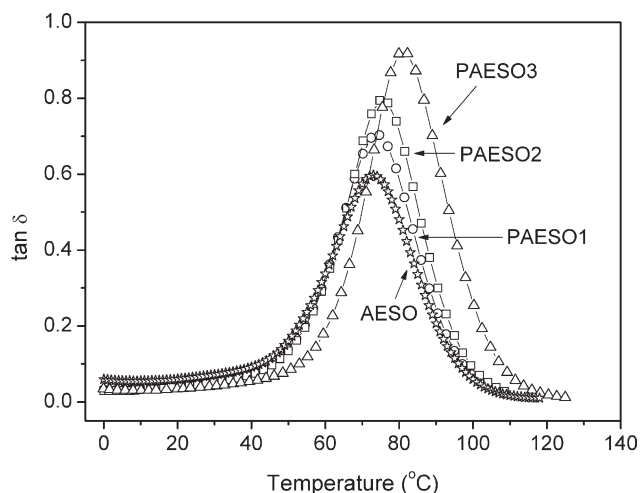
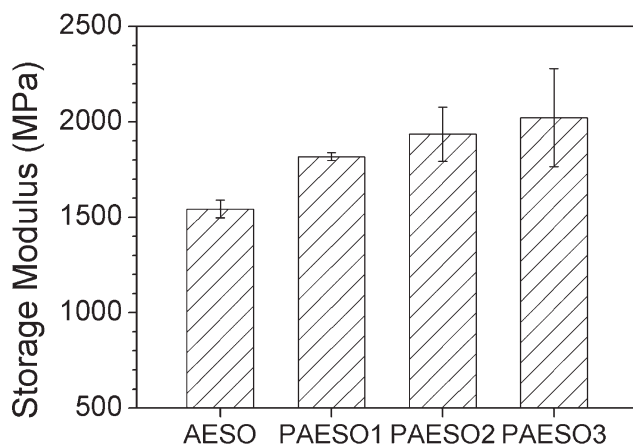


Figure 10 Temperature dependence of $\tan \delta$ of the AESO and PAESOs. The temperatures where the peaks occurred were used as the T_g values.

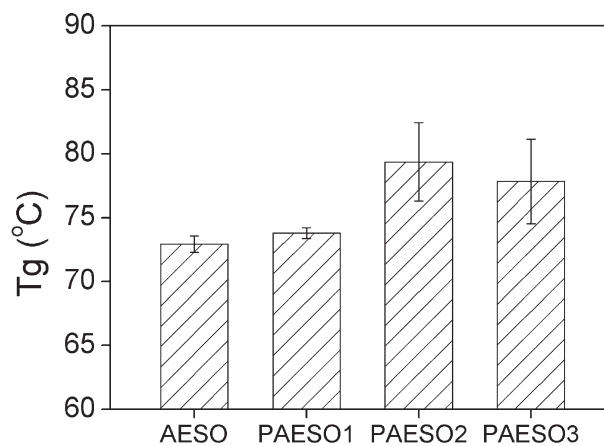
because of the fact that PAESO2 and PAESO3 had very similar molecular weight distributions, in other words, similar compositions and structures.

Figure 10 shows the temperature dependence of $\tan \delta$ for the PAESOs and AESO. With increasing amount PA used, the $\tan \delta$ peak value increased. These peaks corresponded to the moduli drop occurring in the same temperature region (Fig. 9). The shift of the $\tan \delta$ peak to the high-temperature side indicated the increasing rigidity of the molecules, which required higher temperature to start large-scale motion.

The storage moduli of the PAESOs and AESO at 25°C are shown in Figure 11(a). Compared with AESO, PAESO1 had about an 18% increase in modulus, and PAESO2 and PAESO3 had about a 25–30% increase due to the increasing rigidity of the



a



b

Figure 11 (a) Storage modulus of the PAESOs at 25°C. Compared with AESO, PAESO1 had an 18% increase in the modulus, and PAESO2 and PAESO3 had about a 25–30% increase in the modulus. (b) T_g of the PAESOs. The PAESOs had a higher T_g than AESO. However, there was no significant difference between the T_g 's of PAESO2 and PAESO3.

TABLE III
 ϵ Values and Loss Tangents of PAESOs Measured at 1 MHz and Room Temperature

Polymer	ϵ	Loss tangent
AESO	3.77	0.018
PAESO1	3.58	0.0126
PAESO2	3.68	0.0128
PAESO3	3.71	0.0129

polymer structure, as explained by TFT theory. Statistically, however, the moduli of PAESO2 and PAESO3 showed no difference because of the similar molecular structure of PAESO2 and PAESO3.

T_g of PAESO

The T_g values obtained from the peaks of $\tan \delta$ are shown in Figure 11(b). As expected, T_g of PAESO was higher than that of AESO. According to the TFT theory, short rigid side chains resulted in the increase of T_g , which was proven by the results. However, the statistical result shows no difference in the T_g values of PAESO2 and PAESO3, which was consistent with the previous analysis of their molecular structures.

ϵ values of the PAESO polymers

The ϵ values and loss tangents of the PAESO polymers at 1 MHz measured at room temperature are listed in Table III. The ϵ values of these polymers ranged from 3.58 to 3.77 and were lower than the conventional epoxy dielectrics ($\epsilon \approx 4.2\text{--}4.7$). The lower ϵ values make the polymer a potential replacement for petroleum-based dielectric materials. The loss tangents of these materials were lower than 0.02 and are suitable for PCB applications. Given that this biobased material has a much lower carbon dioxide footprint, it is a much greener and environmentally friendly material for the PCB industry and for other applications.

CONCLUSIONS

In this study, two synthetic approaches were used to modify soybean resins to obtain desirable properties, guided by the design rules developed by the ACRES group and others:

1. The equation of predicting the crosslink density in terms of the level of chemical functionalities of the triglycerides was found to be an efficient design rule for high-crosslinked polymer materials.
2. TFT, which predicts linear relationships between T_g and crosslink density of the polymer network, was adopted to design triglyceride resins with suitable T_g values. The resulting T_g of the DVB-crosslinked polymers agreed with the linearity of the TFT of T_g .

3. TFT also suggested the structure effects on the storage modulus of the polymeric materials. The use of a rigid structure to the polymer improved its modulus, which was proven by both approaches in this study.
4. Nonpolar or low-polar comonomer added to the resins resulted in polymers with low ϵ values.
5. The newly developed triglyceride resin systems had higher T_g values, higher moduli, lower ϵ values, and suitable dielectric loss tangents and, thus, have advantages for PCB applications.

The authors thank Alejandrina Campanella for valuable discussions about the synthesis of PAESO. They also thank John Q. Xiao of the Physics Department at the University of Delaware for the use of their HP 4294A Precision Impedance Analyzer.

References

1. Mustafa, N. *Plastics Waste Management: Disposal, Recycling, and Reuse*; Marcel Dekker: New York, 1993.
2. Li, F. K.; Larock, R. C. *J Appl Polym Sci* 2001, 80, 658.
3. Khot, S. N.; Lascalea, J. J.; Can, E.; Morye, S. S.; Williams, G. I.; Palmese, G. R.; Kusefoglou, S. H.; Wool, R. P. *J Appl Polym Sci* 2001, 82, 703.
4. Can, E.; Kusefoglou, S.; Wool, R. P. *J Appl Polym Sci* 2001, 81, 69.
5. Can, E.; Kusefoglou, S.; Wool, R. P. *J Appl Polym Sci* 2002, 83, 972.
6. La Scala, J.; Wool, R. P. *J Am Oil Chem Soc* 2002, 79, 59.
7. La Scala, J.; Wool, R. P. *J Am Oil Chem Soc* 2002, 79, 373.
8. Hong, C. K.; Wool, R. P. *J Appl Polym Sci* 2005, 95, 1524.
9. Wool, R. P.; Sun, X. S. *Bio-Based Materials*; Elsevier Academic: New York, 2005.
10. Wool, R. P. *Soft Matter* 2008, 4, 400.
11. Wool, R. P. *J Polym Sci Part B: Polym Phys* 2008, 46, 2765.
12. Debye, P. *Phys Z* 1912, 13, 97.
13. Li, F.; Hanson, M. V.; Larock, R. C. *Polymer* 2001, 42, 1567.
14. Menard, K. P. *Dynamic Mechanical Analysis: A Practical Introduction*; CRC: Boca Raton, FL, 1999.
15. Ferry, J. D. *Viscoelastic Properties of Polymers*; Wiley: New York, 1980.
16. La Scala, J. J. Ph.D. Dissertation, University of Delaware, 2002.
17. La Scala, J.; Wool, R. P. *Polymer* 2005, 46, 61.
18. Flory, P. J. *Principles of Polymer Chemistry*; Cornell University Press: Ithaca, NY, 1953.
19. Khot, S. Ph.D. Dissertation, University of Delaware, Newark, DE, 2001.
20. Gordon, M.; Roe, R. J. *J Polym Sci* 1956, 21, 75.
21. Loshak, S. *J Polym Sci* 1955, 15, 391.
22. Fox, T. G.; Loshak, S. *J Polym Sci* 1955, 15, 371.
23. DiMarzio, E. A. *J Res Natl Bur Stand Sect A* 1964, 68, 611.
24. Stutz, H.; Illers, K. H.; Mertes, J. *J Polym Sci Part B: Polym Phys* 1990, 28, 1483.
25. Morgen, M.; Ryan, E. T.; Zhao, J. H.; Hu, C. A.; Cho, T. H.; Ho, P. S. *JOM J Miner Met Mater Soc* 1999, 51, 37.
26. Treichel, H.; Withers, B.; Ruhl, G.; Ansmann, P.; Wurl, R.; Muller, C.; Dietlmeier, M.; Maier, G. In *Handbook of Low and High Dielectric Constant Materials and Their Applications*; Nalwa, H. S., Ed.; Academic: San Diego, 1999.
27. Zhan, M.; Wool, R. P. Presented at The 13th Annual Green Chemistry and Engineering Conference, College Park, MD, June 2009.
28. Ku, C. C.; Liepins, R. *Electrical Properties of Polymers: Chemical Principles*; Hanser: New York, 1987.
29. Lanza, V. L.; Herrmann, D. B. *J Polym Sci* 1958, 28, 622.
30. Lu, J.; Hong, C. K.; Wool, R. P. *J Polym Sci Part B: Polym Phys* 2004, 42, 1441.